Aggregation Effect on the Luminescence Properties of Phenylbipyridine Pt(II) Acetylide Complexes. A Theoretical Prediction with Experimental Evidence

ARTICLE *in* THE JOURNAL OF PHYSICAL CHEMISTRY A · JULY 2014

Impact Factor: 2.69 · DOI: 10.1021/jp505764k · Source: PubMed

7 AUTHORS, INCLUDING:

Boixel Julien
French National Centre for Scientific Research

Denis Jacquemin
University of Nantes

Abdou Boucekkine
Université de Rennes 1

THE JOURNAL OF PHYSICAL CHEMISTRY A

Article

pubs.acs.org/JPCA

Aggregation Effect on the Luminescence Properties of Phenylbipyridine Pt(II) Acetylide Complexes. A Theoretical Prediction with Experimental Evidence

Anissa Amar,[†,‡,⊥] Hacène Meghezzi,[‡,⊥] Julien Boixel,[†,⊥] Hubert Le Bozec,[†,⊥] Véronique Guerchais,*[,†] Denis Jacquemin,[§,∥,⊥] and Abdou Boucekkine*[,†]

[†]UMR 6226 CNRS-Université de Rennes 1, Campus de Beaulieu, Institut des Sciences Chimiques de Rennes, 35042 Rennes, France

[‡]Laboratoire de Thermodynamique et Modélisation Moléculaire, USTHB, BP 32 El Alia, 16111 Bab Ezzouar Alger, Algeria

[§]CEISAM, UMR CNRS 6230, Université de Nantes, 44322 Nantes cedex 3, France

[∥]Institut Universitaire de France, IUF, 103, Bd St Michel, F-75005 Paris cedex 5, France

Supporting Information

ABSTRACT: We report a combined theoretical and experimental study of both the structural and optical properties of phosphorescent cyclometalated square-planar (phenylbipyridyl)-platinum(II) acetylide complexes, namely (Pt(tBu$_2$-$\hat{C}\hat{N}N$)(C≡C—Ph)] and (Pt(hex$_2$-$\hat{C}\hat{N}N$)(C≡C—thienyl)] that exhibit, at high concentrations, an additional emission band at longer wavelength. The geometry optimizations of both the ground and the lowest triplet excited states of the considered monomers and different possible dimers have been performed in solution using several density functional theory (DFT) functionals corrected for dispersion effects. For the dimers, which are shown to exhibit a head-to-tail configuration, a significant shortening of the Pt···Pt distance, compared to that in the ground state, is observed in the first triplet state. Moreover, we show that trimeric species are highly improbable in solution. The UV−visible absorption spectra of the complexes are well rationalized using a vertical time-dependent DFT (TD-DFT) protocol relying on a global hybrid exchange−correlation functional. Finally, the new emission band at high concentration of the complexes can be assigned to a metal−metal to ligand charge transfer excited state (^{3}MMLCT).

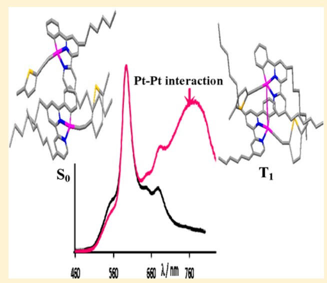

INTRODUCTION

Square-planar platinum(II) polypyridine complexes, presenting a strong tendency toward oligomer formation, have attracted a long-standing attention due to their interesting photophysical properties.[1] Their particular luminescent properties (^{3}MMLCT, metal−metal to ligand charge transfer and/or excimeric excited states), associated with the presence of Pt···Pt and/or π···π stacking interactions[2] have found applications in OLEDs[3] and NIR luminescent probes.[4] The propensity for platinum(II) complexes of engaging metal−metal interactions has been extensively studied, starting with the seminal investigations on terpyridine platinum(II) complexes.[5] Interestingly, the formation of oligomers can be controlled by several parameters, e.g., the temperature, the nature of the counterion, and/or the media.[6] Cyclometalated platinum(II) complexes that show intense phosphorescence at ambient temperature were also studied for their tendency to form aggregates.[7] However, despite the large number of experimental studies on platinum(II) oligomers, only very few theoretical investigations have, to the best of our knowledge, appeared.[8]

Our groups have been exploring the chemistry of cyclometalated ($\hat{C}\hat{N}N$) platinum(II) acetylide complexes as optical chemosensors.[9] In the present work, we now consider the two platinum complexes, Pt(tBu$_2$-$\hat{C}\hat{N}N$)(C≡C—Ph), **1**, and Pt(hex$_2$-$\hat{C}\hat{N}N$)(C≡C—thienyl), **2** (Scheme1), which are likely to exhibit aggregation and interesting photophysical properties. Experimentally, their UV−visible and luminescence spectra have been studied at different concentrations in solution. Theoretically, because the species under consideration are expected to lead to a Pt···Pt associations, geometry optimizations of both the monomers and the "dimeric" complexes have been performed with a DFT approach including both dispersion corrections and solvent effects (see Computational Details). Then, TD-DFT computations have been carried out to assign the absorption and emission bands. The influence of the presence of *tert*-butyl and *n*-hexyl groups of the cyclometalated $\hat{C}\hat{N}N$ ligands is also discussed below; the sterically demanding *tert*-butyl groups could inhibit[10] or not[11,6b] the self-assembling process.

RESULTS AND DISCUSSION

Structures and Geometries. Phenylbipyridine ($\hat{C}\hat{N}N$) platinum(II) acetylide complexes under consideration are depicted in Scheme 1. First, we optimized the geometries of both complexes **1** and **2** in their ground (S$_0$) and lowest triplet excited states (T$_1$) using BLYP-D computations (see Computa-

Received: June 10, 2014
Revised: July 24, 2014
Published: July 31, 2014

Scheme 1. Structures of the Cyclometalated Platinum(II) Complexes 1 and 2

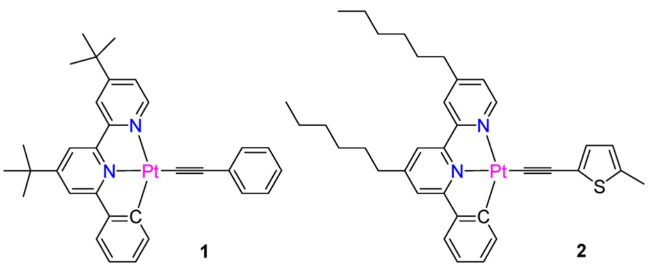

tional Details). Then, dimer structures of the two complexes have been built starting from the ground-state optimized geometries, considering both *syn* (head-to-head) and *anti* (head-to-tail) conformations (see Figure 1 for **dimer-1**). At the same level of theory, we fully optimized the geometries of the **dimers-1** and **-2** in both their S_0 and in T_1 states. The optimized S_0 and T_1 structures of the dimers are presented in Figures 1 and 2. In addition, selected structural and energetic parameters are listed in Table 1.

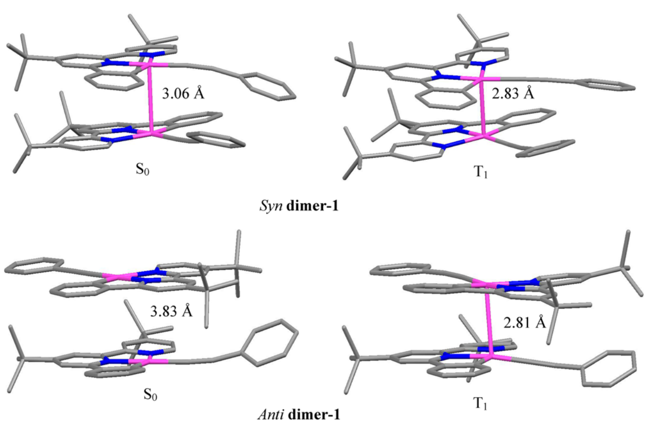

Figure 1. BLYP-D/DZP optimized ground-state (S_0) and lowest triplet excited-state (T_1) geometries with Pt···Pt distances of the Pt(*t*Bu$_2$-ĈN̂N)(C≡C—Ph) dimers. Hydrogen atoms are omitted for clarity.

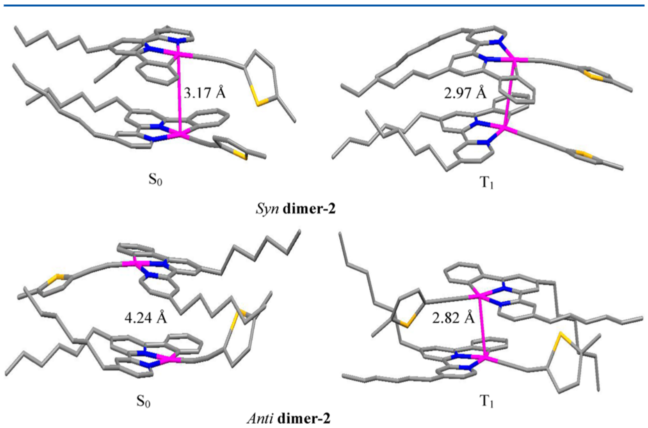

Figure 2. BLYP-D/DZP optimized ground-state (S_0) and lowest triplet excited-state (T_1) geometries with Pt···Pt distances of the Pt(hex$_2$-ĈN̂N)(C≡C—thienyl) dimers. Hydrogen atoms are omitted for clarity.

In our study, we also investigate the stability of the two possible isomers 1 and 2 of both *syn* and *anti* **dimer-1** (Figure S1, Supporting Information). The obtained results indicate that the energies of the two isomers are almost the same (energy difference equal to ca. 0.2 kcal/mol). Note that in our computational study we considered the most stable isomers, i.e., isomer 1 for the *syn* **dimer-1** and isomer 2 for the *anti*, and the given results are only valid for these isomers.

Ground-State Optimized Geometries. Considering the ground-state optimized geometries of dimers of complexes **1** and **2**, it can be seen that both the bond lengths and the valence angles remain close to their monomeric values. For example, the Pt_1-N_2 bond of complex **1** is calculated to be equal to 2.19 Å for the monomer whereas it is 2.18, 2.16 Å and 2.18, 2.17 Å in the two units constituting the *syn* and *anti* **dimer-1**, respectively (Table S1, Supporting Information). Considering the acetylide part of the ligands, which can be affected by dimerization, we note that the Pt_1-C_5, C_5-C_6, and C_6-C_7 distances in the monomer and in the *syn* and *anti* dimers in complex **1** are the same (up to 0.01 Å) that is 1.96, 1.23, and 1.41 Å, respectively. The calculated bond angles in the acetylide part of the complex **1** are weakly affected by aggregation. Indeed, from Table S1 (Supporting Information) we can note that the $Pt_1-C_5-C_6$ angle is equal to 177.8° in the monomer, 169−172° in the *syn* dimer, and 175°−176° in the *anti* one. However, dimerization has a non-negligible effect on dihedral angles especially for the Pt−acetylide moiety (Tables S1 and S2, Supporting Information). These geometric deformations arise from the interplay between Pt···Pt bimetallic interactions and the interligand $\pi\cdots\pi$ interactions.[8]

We first discuss the optimized ground-state geometries of complex **1**. The calculated *syn* conformation of **dimer-1** exhibits a Pt···Pt distance of 3.06 Å that is significantly smaller than the sum of van der Waals' radii of the Pt atoms (3.4 Å), suggesting a significant intermolecular interaction between the two metal centers. For the same conformation, the calculated average interplanar distances between the ĈN̂N ligands equals 3.21 Å. For this *syn* conformation, the two ĈN̂N ligands are in a staggered conformation, which minimizes the repulsion between the bulky *tert*-butyl groups. Both the Pt···Pt interaction and the $\pi\cdots\pi$ stacking interactions in this *syn* conformation of **dimer-1** are the driving factors associating the Pt *t*Bu$_2$-ĈN̂N units together. We also underline that the two monomers constituting the *syn* **dimer-1** are distorted from planarity to accommodate the Pt···Pt interaction.

As the dipole moment of complex **1** is large (15.6 D), a head-to-tail stacking is expected. Indeed, our computations indicate that the *anti* dimer is more stable than its *syn* counterpart by 13 kcal.mol^{-1}. Nevertheless, a significantly longer Pt···Pt distance of 3.83 Å is surprisingly obtained for the *anti* **dimer-1** than for the *syn* conformer (3.06 Å). We can see from Figure 1 that in the *anti* conformation, one of the monomers is displaced with respect to the other and this allows the two ĈN̂N parts to be parallel, with an average distance of 3.52 Å, a nearly ideal situation for a $\pi-\pi$ interaction. This indicates that interligand $\pi-\pi$ interactions play an important role in the stability of the ground-state dimer structure, and that Pt···Pt interactions are not the unique driving force. As can be seen from Figures 1 and 2, the acetylide ligands in the *syn* optimized structures are not parallel, and the calculated average interplane distance between them equals 3.76 and 3.91 Å for complexes **1** and **2**, respectively, contrary to the ĈN̂N ligands that adopt a face-to-face configuration in the *syn* and *anti* dimers, at a mean

dx.doi.org/10.1021/jp505764k | J. Phys. Chem. A 2014, 118, 6278−6286

Table 1. Selected S_0 and T_1 Optimized Geometric Parameters and Energies of the Considered Monomers and Dimers

	S_0			T_1		
	monomer	*syn* dimer	*anti* dimer	monomer	*syn* dimer	*anti* dimer
Complex 1						
energy (eV)[a]	−405.27	−813.15	−813.74	−403.23	−811.70	−811.90
d(Pt···Pt) (Å)		3.06	3.83		2.83	2.81
d((ĈN̂N)···(ĈN̂N)] (Å)		3.21	3.52		3.14	4.04
θ(N2−Pt1−Pt1′−N2′) (deg)		32.27	146.71		32.54	136.77
Complex 2						
energy (eV)[a]	−462.59	−928.05	−928.55	−460.86	−926.75	−926.98
d(Pt···Pt) (Å)		3.17	4.24		2.97	2.82
d((ĈN̂N)···(ĈN̂N)] (Å)		3.21	3.14		3.20	3.92
θ(N2−Pt1−Pt1′−N2′) (deg)		34.38	128.17		38.00	130.88

[a]Total binding energy (TBE).

distance of 3.21 and 3.52 Å for complex **1**, and 3.21 and 3.14 Å for complex **2** (Table 1). Moreover, in the most stable *anti* dimers, the acetylides adopt trans configurations. Thus, we can reasonably state that the interaction between the two acetylide ligands in the dimers should be smaller than the interaction beween the phenylbipyridyl moieties.

Let us now consider the dimer of complex **2**: its optimized S_0 geometries in both *syn* and *anti* conformations show longer Pt···Pt distances compared to those of complex **1**. Indeed, this distance attains 3.17 and 4.24 Å for the *syn* and *anti* dimers, respectively. The two ĈN̂N ligands in both *syn* and *anti* geometries adopt the same conformation as the one obtained for the **dimers-1** (Figure 2). The calculated average interplanar distances between the ĈN̂N ligands are equal to 3.21 and 3.14 Å for the *syn* and *anti* conformers, respectively, indicating favorable $\pi\cdots\pi$ stacking interactions and confirming the important role of these interactions in ground-state structures. In addition, the *anti* **dimer-2** is calculated to be more stable than the *syn* one by 11 kcal.mol^{-1}, a result that is consistent with the large ground-state dipole moment of **2** (15.41 D).

Triplet-State Optimized Geometries. Optimization of the lowest triplet excited state (T_1) of the dimer of complex **1** indicates several distortions, especially of the dihedral angles (Tables S1 and S2, Supporting Information). It is expected that the structure of a possible dimeric excimer differs significantly from the ground state of the dimer as it has been shown that diplatinum compounds can display an important decrease of the Pt···Pt distance upon excitation.[12] Indeed, the T_1 geometry optimization of **dimer-1** leads to a shortening of the Pt···Pt distance compared to the case for S_0 (2.83 Å vs 3.06 Å for *syn* and 2.81 Å vs 3.83 Å for *anti*). In the *anti* T_1 state of **dimer-1**, the two monomers adopt a conformation in favor of the Pt···Pt interaction, keeping the two ĈN̂N ligands distant from each other, thus diminishing the $\pi\cdots\pi$ stacking interactions. Indeed, the calculated average distance between the two ĈN̂N moieties in the *anti* conformation is equal to 4.04 Å. In short, the Pt···Pt interaction in the *anti* **dimer-1** is weak in S_0 but large in T_1.

Dimers-2 exhibit a similar behavior when going from S_0 to T_1 (Pt···Pt going from 3.17 to 2.97 Å for the *syn* conformer and from 4.24 to 2.82 Å for the *anti* conformer). In addition, the average distance between the two phenylbipyridine ligands is 3.20 and 3.92 Å for the *syn* and *anti* conformations of the T_1 **dimer-2** respectively.

We highlight that both complexes **1** and **2** lead to contraction of the Pt···Pt distance upon excitation; the presence of *tert*-butyl and hexyl substituents on the ĈN̂N ligand does not inhibit the attractive interactions between two organometallic units.

To check the reliability of the obtained results, we have also performed geometry optimizations using other dispersion corrected functionals, namely, ωB97X-D and PBE0-D3 combined with the LANL2DZ basis set augmented with polarization functions on all nuclei, except the hydrogen atoms and taking into account the solvent CH_2Cl_2 (see Computational Details). Moreover, the basis set has been further extended with diffuse orbitals when the PBE0-D3 functional is used. Selected geometric parameters and energies of the monomer and dimers at the different levels of computation are listed in Table S3 (Supporting Information). In addition, the emission energies calculated at the PBE0-D3/LANL2DZP level are given in Table S4 (Supporting Information).

The obtained optimized geometries of complex **1** and its dimers, using the ωB97X-D and PBE0-D3 functionals, are similar to those obtained using BLYP-D computations. Indeed, the stability of the *anti* **dimer-1** compared to that of the *syn* one (Table S3, Supporting Information) in the ground state is confirmed. The same applies to the geometries of the triplet states; for instance, the PBE0-D3/LANL2DZP lowest triplet excited-state (T_1) geometry optimization of **dimer-1** leads to a shortening of the Pt···Pt distance compared to the case for S_0 (2.81 Å vs 3.36 Å for *syn* and 2.79 Å vs 4.07 Å for *anti*) (Table S3, Supporting Information) similar to the BLYP-D prediction. The addition of diffuse orbitals to the LANL2DZP basis set led only to a slight variation of these distances.

To investigate the possible existence of trimeric species in solution, either in the ground or in the triplet states, we carried out geometry optimizations for such species using the same theoretical scheme as for the monomer and dimer. In the case of complex **1**, the initial geometry was formed starting from an optimized dimer to which a third complex has been attached at a short Pt···Pt distance of 3.00 Å. Moreover, the three complexes constituting the starting geometry of the trimeric species have been arranged in the favored *anti* conformation. The ground-state full geometry optimization at the PBE0-D3/LANL2DZP level led us to three separated complexes, with Pt···Pt distances equal to 3.92 and 4.00 Å (Figure S4, Supporting Information), whereas in the triplet state a dimer exhibiting a Pt···Pt distance equal to 2.80 Å is obtained, the third complex being repelled at a Pt···Pt distance of 3.89 Å (Figure S4, Supporting Information) by the force minimization process. To conclude, the formation of trimeric species in solution is highly improbable, whereas the existence of dimeric aggregates in the triplet state is confirmed.

■ PHOTOPHYSICAL STUDIES OF THE COMPLEXES

UV–Visible Absorption. The UV–visible absorption spectra of **1** and **2** measured in dichloromethane at 298 K are presented in Figure 3, whereas the characteristic data are collected in Table 2. The observed absorption spectra of complex **1** at different concentrations are depicted in Figure S5 in the Supporting Information, together with the corresponding excitation spectrum. The observed absorption spectra of complexes **1** and **2** exhibit an intense absorption band in the UV region (λ = 300–380 nm) and an absorption band at ca. 430 (**1**) and 460 (**2**) nm. Compared to the case for **1**, a red shift of 30 nm of the low-energy absorption band is therefore observed for **2**.

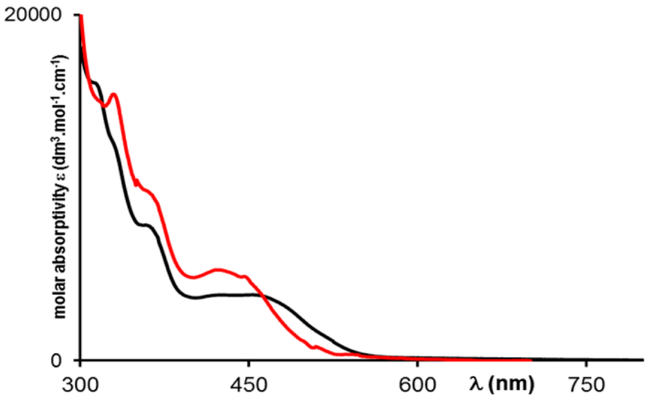

Figure 3. Measured absorption spectra of complexes **1** (red line) and **2** (black line) at 298 K in CH_2Cl_2, $C \approx 10^{-5}$ M.

Table 2. Measured Absorption Data for Complexes 1 and 2 in CH_2Cl_2

compound	λ_{abs}^{a}/nm (ε x10^3/dm^3 mol^{-1} cm^{-1})^{a}
1	320 (15.1), 360 (9.8), 430 (5.1)
2	320 (14.9), 360 (7.8), 460 (3.9)

[a] At 298 K in 2.5 × 10^{-5} M.

Starting from the optimized geometries obtained at the BLYP-D/DZP level in CH_2Cl_2, the TD-PBE0/LANL2DZP level has been performed to simulate the UV–visible spectra of complexes **1** and **2** in dichloromethane. The computed vertical absorption spectra of the monomer and dimers are displayed in Figure 4, and the calculated absorption wavelengths are reported in Table 3. In addition, the MOs involved in the related electronic transitions are shown in Figure S2 and S3 in the Supporting Information.

The simulated UV–vis spectra of the monomer and dimers of complex **1** display a low-energy absorption in the visible region assigned to a mixture of L′LCT from alkynyl-to-phenylbipyridine [π(alkynyl) → π^*(ĈN̂N)] and of metal-to-ligand charge transfer (MLCT) [dπ(Pt) → π^*(ĈN̂N)]. Interestingly, the *syn* **dimer-1** exhibits an additional lower energy absorption band at 599 nm, red-shifted by 158 and 161 nm, compared to the case of the corresponding monomer and *anti* dimer, respectively. Experimentally, upon increasing the concentration of complex **1** (from 8.1 × 10^{-5} to 1.3 × 10^{-3} M) no new red-shifted absorption band is observed (Figure S5, Supporting Information). This experimental observation is, however, not surprising because the most stable form of **dimer-1** is the *anti* (not the *syn* conformer) that does not display an additional absorption band at lower energy. The calculated new low energy absorption band for the *syn* **dimer-1** is assigned to a combination of L′LCT and MLCT from the HOMO localized on the Pt–acetylide (that presents considerable weights of the two Pt atoms, 30.28% and 31.77%), to the LUMO delocalized on the ĈN̂N ligand. Let us recall that the optimized *syn* **dimer-1** exhibits a short Pt···Pt contact of 3.06 Å in the ground state.

From Figure 4b, it can be seen that the simulated UV–vis spectra of the dimers of complex **2** are not strongly affected by the conformation. The absorption in the visible for both the monomer and the dimers of complex **2** arises from a blend of L′LCT and MLCT from the Pt–acetylide and the adjacent thiophene toward the bipyridine moiety of the ĈN̂N ligand. The calculated absorption is red-shifted by 13 and 50 nm for the *syn* dimer compared to the absorptions for the monomer and *anti* dimer, respectively.

With the aim of gaining more insights into the origin of the additional lower energy absorption band calculated for the *syn* **dimer-1**, we further performed TD-DFT calculation on this latter species considering several Pt···Pt distances starting from the previously S_0 optimized geometry. The obtained spectra versus the Pt···Pt distances are depicted in Figure 5. Obviously, the simulated spectra of the *syn* **dimer-1** at larger Pt···Pt

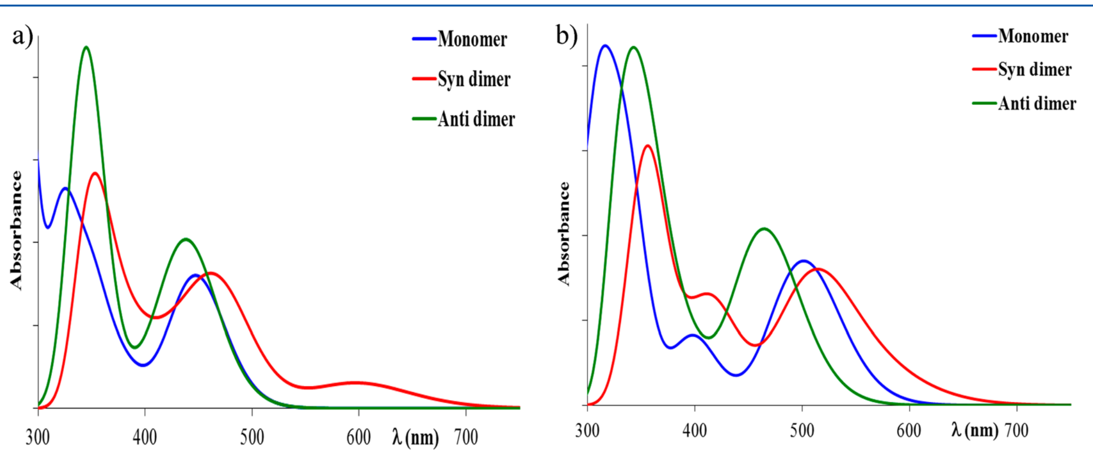

Figure 4. Simulated UV–visible spectra of complexes (a) **1** and (b) **2** at the PBE0/LANL2DZP level in CH_2Cl_2: monomer (blue line), *syn* dimer (red line), and *anti* dimer (green line).

Table 3. Calculated Absorption Spectra (λ_{max} in nm and Oscillator Strengths in au) at the PBE0/LANL2DZP Level in CH_2Cl_2[a]

compound	λ_{max}	λ_{calc}	f	main contributions (weight)	assignment
			Complex **1**		
monomer	324	323	0.2258	HOMO−4 → LUMO(+81%)	ILCT/MLCT
	441	448	0.2163	HOMO → LUMO(+96%)	L′LCT/MLCT
syn dimer	351	348	0.1304	HOMO−7 → LUMO(+64%)	ILCT/MLCT
	467	470	0.1210	HOMO−1 → LUMO+1(+75%)	L′LCT/MLCT
	599	599	0.0415	HOMO → LUMO(+92%)	L′LCT/MLCT
anti dimer	345	344	0.2300	HOMO−1 → LUMO+3(+44%)	L′LCT/MLCT
				HOMO−3 → LUMO+2(+18%)	ILCT/MLCT
	438	444	0.1679	HOMO → LUMO+1(+59%)	L′LCT/MLCT
			Complex **2**		
monomer	316	312	0.2626	HOMO → LUMO+3(+50%)	ILCT/MLCT/L′LCT
				HOMO−6 → LUMO(44%)	
	398	400	0.1023	HOMO → LUMO +1(+97%)	L′LCT/MLCT
	502	501	0.2344	HOMO → LUMO(+98%)	L′LCT/MLCT
syn dimer	356	360	0.1922	HOMO−3 → LUMO+2(+59%)	ILCT/MLCT
				HOMO−4 → LUMO+2(+21%)	
	411	415	0.0784	HOMO−6 → LUMO(+36%)	L′LCT/MLCT
				HOMO−5 → LUMO(29%)	
	515	512	0.1492	HOMO−1 → LUMO+1(+73%)	L′LCT/MLCT
anti dimer	342	330	0.1885	HOMO−1 → LUMO+4(+38%)	L′LCT/MLCT
				HOMO → LUMO+4(+31%)	
	465	461	0.1142	HOMO → LUMO+1(+61%)	L′LCT/MLCT

[a] λ_{calc} are the vertical TD-DFT absorption wavelengths. The weight of each MO contribution in the excitation is also given.

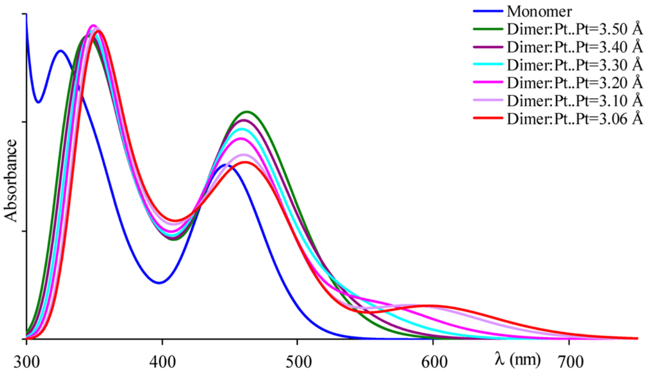

Figure 5. Simulated absorption spectra of complex *syn* **dimer-1** [Pt(tBu$_2$-ĈN̂N)(C≡C—Ph)] as a function of the Pt···Pt distance.

distance (3.50 and 3.30 Å) are similar to that of the monomer spectrum. However, at a distance of 3.20 Å between the two platinum atoms the UV−visible spectrum of the **dimer-1** displays additional shoulder at ca. 530 nm. When the two platinum atoms come closer, this new absorption band becomes more intense and is red-shifted.

Emission Spectroscopy. Upon excitation at 430 nm, complex **2** displays luminescence centered at 595 nm with an associated quantum yield Φ_{lum} of 0.03 (CH_2Cl_2, 298 K). The emission spectrum has a broad, structureless profile that depends on the concentration (Figure 6b): increasing the concentration, from 10^{-5} to 10^{-4} M, leads to the formation of a new strongly red-shifted emission band at 770 nm. A similar behavior is found for complex **1**, the newly formed emission band is located at 640 nm whereas the band of (the remaining) monomer becomes less intense and is slightly blue-shifted to 540 nm. This result demonstrates that the presence of bulky *tert*-butyl substituents on the ĈN̂N ligand does not inhibit the interactions between two organometallic units.

First, let us remember that the *anti* form remains more stable than the *syn* conformer in the T_1 state (Table 1). The PBE0/LANL2DZP calculated $T_1 \rightarrow S_0$ emission energy for the

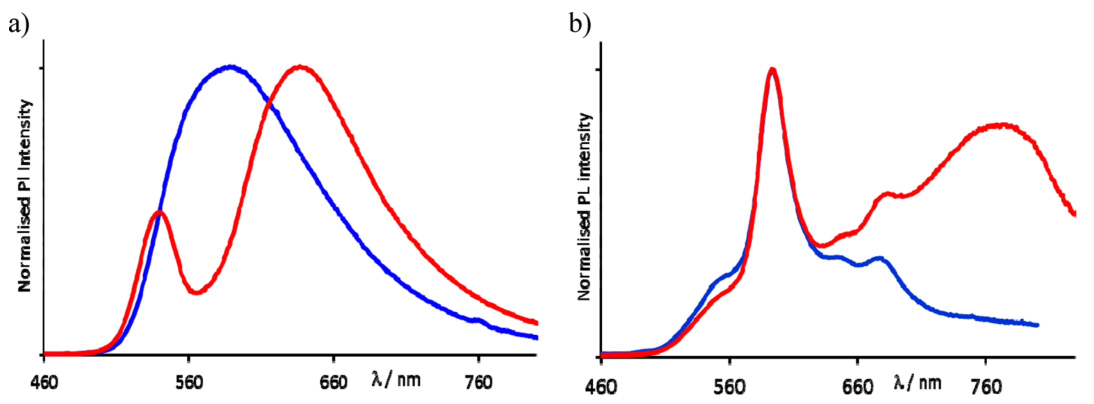

Figure 6. Emission spectra (λ_{ex} = 430 nm, CH_2Cl_2) of (a) **1** and (b) **2** at 298 K. $C \approx 10^{-5}$ M (blue line) and $C \approx 10^{-4}$ M (red line).

Table 4. Experimental (Exp) and Calculated (Calc) Emission Data for the Monomer and Dimers of 1 and 2

	λ_{em}/nm (E_{em}/eV)				
	exp[a,b]		calc		
	$C \approx 10^{-5}$ M	$C \approx 10^{-4}$ M	monomer	*syn* dimer	*anti* dimer
1	590 (2.10)	540 (2.30), 640 (1.93)	607 (2.04)	855 (1.45)	674 (1.84)
2	595 (2.08), 670 (1.85)	595 (2.08), 670 (1.85), 770 (1.61)	716 (1.73)	951 (1.30)	790 (1.57)

[a]At 298 K in 2.5×10^{-5} M. [b]λ_{ex} = 430 nm.

monomer of **1** is 2.04 eV (Table 4), in excellent agreement with the experimental data at 10^{-5} M (2.10 eV). Experimentally, at 10^{-4} M, a new emission at lower energy is observed for complex **1** at about 1.93 eV. For the *syn* (*anti*) conformation the theoretical emission energy is 1.45 eV (1.84 eV), indicating a difference of emission energy of 0.6 eV (0.2 eV) with respect to the monomer. We note that the calculated $T_1 \rightarrow S_0$ emission energy for the *anti* conformation nicely matches the observed emission at 10^{-4} M, whereas the one calculated for the *syn* dimer is significantly smaller than the experimental value at the same concentration. We observe the same good agreement between the observed and computed emission energies for complex **2**. Besides, for complexes **1** and **2**, the frontier MOs for *syn* geometry have the same nature for both the S_0 and T_1 states. On the contrary, while the HOMO of the S_0 *anti* geometry is localized on the Pt−acetylide part, it becomes spectacularly centered on the two Pt atoms (Tables 5 and 6)

Table 5. Frontier MOs at the Isovalue of 0.03 au for the *Syn* and *Anti* Dimers of Pt(tBu$_2$-ĈN̂N)(C≡C—Ph) (1) Considering the S_0 and T_1 Optimized Geometries

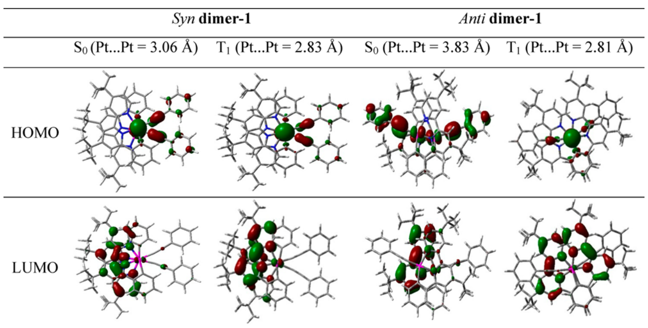

Table 6. Frontier MOs at the Isovalue of 0.03 au for the *Syn* and *Anti* Pt(hex$_2$-ĈN̂N)(C≡C—thienyl) (2) Considering the S_0 and T_1 Optimized Geometries

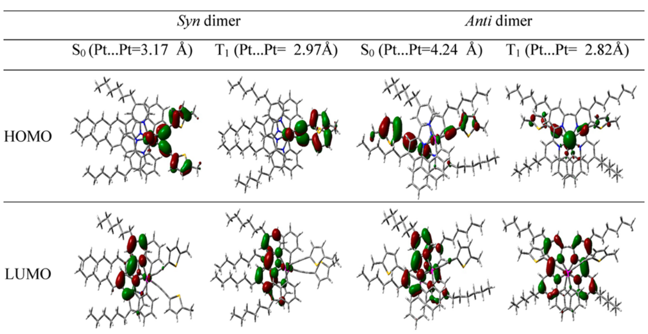

for the T_1 state, the *anti* LUMOs remaining centered on the bipyridine moiety of the ĈN̂N ligand. Consequently, we can conclude that the observed lower emission energy in concentrated solution comes from the *anti* excimer-like dimer and originates from metal−metal to ligand charge transfer (^{3}MMLCT), the latter triplet state being characterized by strong the Pt···Pt interaction.

Furthermore, $T_1 \rightarrow S_0$ emission energies computed for complex **1** at the PBE0-D3/LANL2DZP level in CH_2Cl_2 are similar to those obtained at the BLYP-D level (Table S4, Supporting Information). The PBE0-D3 calculated emission energy for the monomer of complex **1** (2.19 eV) is in good agreement with the measured data at 10^{-5} M (2.10 eV). In addition, the calculated emission energy for the *anti* **dimer-1** (1.87 eV) nicely matches the observed emission at 10^{-4} M (1.93 eV). It is interesting to notice that the emission energy calculated for the *syn* dimer (1.60 eV) is smaller than the observed value at the same concentration, thus hinting that this species does not exist in this solution.

■ CONCLUSIONS AND OUTLOOK

In this work we have reported the results of combined theoretical and experimental investigations of (Pt(tBu$_2$-ĈN̂N)-(C≡C—Ph)] and (Pt(hex$_2$-ĈN̂N)(C≡C—thienyl)], two phosphorescent cyclometalated platinum(II) acetylide complexes. The ground-state DFT-D geometry optimizations for the two considered platinum complexes **1** and **2** indicate that (i) considering the formation of dimeric species, the *anti* conformation (head-to-tail) is favored over the *syn* one (head-to-head); (ii) interligand $\pi-\pi$ stacking interactions play an important role; and (iii) the formation of trimeric species is highly improbable in solution. The lowest triplet excited calculated geometries of both **dimers-1** and **-2** in their *syn* and *anti* conformations exhibit a significant shortening of the Pt···Pt distance, likely to indicate the formation of an excimer-like dimer, the presence of a bulky *tert*-butyl substituent on the ĈN̂N ligand not inhibiting the attractive interactions between two organometallic units. The simulated UV−visible spectra of the most stable *anti* **dimer-1** show negligible variations compared to the spectra for its monomeric counterpart. On the contrary, the *syn* **dimer-1** would exhibit a new absorption band at lower energy resulting from Pt···Pt distance shortening. More importantly, both complexes exhibit a new low energy emission band in concentrated solutions that can be assigned to a metal−metal to ligand charge transfer (^{3}MMLCT) excited state of the *anti* dimer, and the calculated $T_1 \rightarrow S_0$ emission energies are in good agreement with experiment.

■ COMPUTATIONAL DETAILS

The geometry optimizations of the complexes have been performed using the Amsterdam Density functional (ADF) program.[13] The BLYP[14] exchange−correlation functional with the Grimme's dispersion correction,[15] i.e., the BLYP-D, was used, in combination with the DZP basis set for all elements, within the zeroth-order regular approximation (ZORA)[16] at the scalar relativistic level. In the case of the BLYP-D computations, solvation effects were modeled by the conductor-like screening model (COSMO)[17] considering dichloromethane as solvent. The optimized geometries of monomers and dimers were used to perform TD-DFT calculations at the PBE0[18] level using the LANL2DZ[19] basis set augmented with polarization functions (D exponent for C, N, and S, i.e., 0.5870, 0.7360, and 0.4960, respectively, and F exponent for Pt, i.e., 0.8018, the new basis set being denoted LANL2DZP) on all atoms, except hydrogen ones, with the Gaussian09 program.[20] In the TD-DFT calculations, the solvent effects were taken into account by means of the polarizable continuum model (PCM).[21] Theoretical emission energies were calculated as the difference between the energies of the optimized species in the ground (S_0) and lowest triplet excited states (T_1). Drawings of molecular structures were done using the Mercury software,[22] and molecular orbitals using GaussView[23] program, whereas theoretical absorption spectra were plotted using Swizard.[24] Percentage compositions of molecular orbitals (MOs) were analyzed using the AOMix[25] program.

To check the reliability of the obtained theoretical results, we also performed geometry optimizations using two other dispersion corrected functionals, namely ωB97X-D[26] and PBE0-D3[15] combined with the LANL2DZ basis set augmented with polarization functions on all nuclei, except the hydrogen atoms, taking into account the solvent CH_2Cl_2. Moreover, the LANL2DZP has also been further extended with diffuse orbitals (p exponent for C and N, respectively, 0.0311 and 0.0533; d exponent for Pt, 0.0188) when the PBE0-D3 functional is used.

■ ASSOCIATED CONTENT

Ⓢ Supporting Information

Optimized S_0 geometries of the dimers, structures of **1** and **2**, relevant molecular orbitals, selected S_0 and T_1 optimized geometric parameters, emission data for **1**, S_0 and T_1 geometries of the trimers, experimental section for the synthesis of the complexes, absorption, excitation, and emission spectra, and Cartesian coordinates of complexes **1** and **2**. This material is available free of charge via the Internet at http://pubs.acs.org.

■ AUTHOR INFORMATION

Corresponding Authors

*V. Guerchais. E-mail: veronique.guerchais@univ-rennes1.fr.
*A. Boucekkine. E-mail: abdou.boucekkine@univ-rennes1.fr.

Notes

The authors declare no competing financial interest.

⊥E-mail: A. Amar, anissa.haddad@univ-rennes1.fr; H. Meghezzi, hmeghezzih@yahoo.fr; J. Boixel, julien.boixel@univ-rennes1.fr; H. Le Bozec, hubert.le-bozec@univ-rennes1.fr; D. Jacquemin, denis.jacquemin@univ-nantes.fr.

■ ACKNOWLEDGMENTS

This research used resources of (1) the GENCI-IDRIS-CINES National Computing Centers and (2) CCIPL (Centre de Calcul Intensif des Pays de la Loire. D. Jacquemin acknowledges both the European Research Council (ERC) and the *Région des Pays de la Loire* for financial support in the framework of a Starting Grant (Marches 278845) and *recrutement sur poste stratégique*, respectively.

■ REFERENCES

(1) (a) Williams, J. A. G. Photochemistry and Photophysics of Coordination Compounds: Platinum. *Top. Curr. Chem.* **2007**, *281*, 205−268. (b) Williams, J. A. G.; Develay, S.; Rochester, D. L.; Murphy, L. Optimising the Luminescence of Platinum(II) Complexes and Their Application in Organic Light Emitting Devices (OLEDs). *Coord. Chem. Rev.* **2008**, *252*, 2596−2611. (c) Williams, J. A. G. The Coordination Chemistry of Dipyridylbenzene: N-Deficient Terpyridine or Panacea for Brightly Luminescent Metal Complexes? *Chem. Soc. Rev.* **2009**, *38*, 1783−1801. (d) Yersin, H.; Donges, D. Low-Lying Electronic States and Photophysical Properties of Organometallic Pd(II) and Pt(II) Compounds. Modern Research Trends Presented in Detailed Case Studies. *Top. Curr. Chem.* **2001**, *214*, 81−186. (e) Lai, S. W.; Che, C. M. Luminescent Cyclometalated Diimine Platinum(II) Complexes: Photophysical Studies and Applications. *Top. Curr. Chem.* **2004**, *241*, 27−63. (f) Kato, M. Luminescent Platinum Complexes Having Sensing Functionalities. *Bull. Chem. Soc. Jpn.* **2007**, *80*, 287−294. (g) Wong, K. M.-C.; Yam, V. W.-W. Luminescent Metal Complexes of d^6, d^8 and d^{10} Transition Metal Centres. *Chem. Commun.* **2011**, *47*, 11579−11592.

(2) (a) Lu, W.; Mi, B. X.; Chan, M. C. W.; Hui, Z.; Che, C. M.; Zhu, N.; Lee, S. T. Light-Emitting Tridentate Cyclometalated Platinum(II) Complexes Containing ó-Alkynyl Auxiliaries: Tuning of Photo-and Electrophosphorescence. *J. Am. Chem. Soc.* **2004**, *126*, 4958−4971. (b) Anderson, B. M.; Hurst, S. K. Platinum Stacking Interactions in Homoleptic Platinum Polymers. *Eur. J. Inorg. Chem.* **2009**, *21*, 3041−3054. (c) Utsono, M.; Yutaka, T.; Murata, M.; Kurihara, M.; Tamai, N.; Nishihara, H. Synthesis of Pendant-Type Anthraquinone-Bridged Cofacial Dinuclear Platinum(II) Complexes and Their Emission Properties. *Inorg. Chem.* **2007**, *46*, 11291−11296. (d) Yam, V. W. W.; Chan, K. H. Y.; Wong, K. M. C.; Zhu, N. Luminescent Platinum(II) Terpyridyl Complexes: Effect of Counter Ions on Solvent-Induced Aggregation and Color Changes. *Chem.—Eur. J.* **2005**, *11*, 4535−4543. (e) Lai, S. W.; Lam, H. W.; Lu, W.; Cheung, K. K.; Che, C. M. Observation of Low Energy Metal-Metal-to-Ligand Charge Transfer Absorption and Emission: Electronic Spectroscopy of Cyclometalated Platinum(II) Complexes with Isocyanide Ligands. *Organometallic* **2002**, *21*, 226−234. (f) Ding, J.; Pan, D.; Tung, C. H.; Wu, L. Z. Synthesis and Photophysical Studies of Calix[4]Arene-Based Binuclear Platinum(II) Complexes: Probing Metal-Metal and Ligand-Ligand Interactions. *Inorg. Chem.* **2008**, *47*, 5099−5106. (g) Lu, W.; Chan, M. C. W.; Cheung, K. K.; Che, C. M. π-π Interactions in Organometallic Systems. Crystal Structures and Spectroscopic Properties of Luminescent Mono-, Bi-, and Trinuclear Trans-Cyclometalated Platinum(II) Complexes Derived from 2,6-Diphenylpyridine. *Organometallics* **2001**, *20*, 2477−2486. (h) Lai, S. W.; Chan, M. C. W.; Cheung, K. K.; Che, C. M. Carbene and Isocyanide Ligation at Luminescent Cyclometalated 6-Phenyl-2,2′-bipyridyl Platinum(II) Complexes: Structural and Spectroscopic Studies. *Organometallics* **1999**, *18*, 3327−3336. (i) Lu, W.; Chan, M. C. W.; Zhu, N.; Che, C. M.; Li, C.; Hui, Z. Structural and Spectroscopic Studies on Pt···Pt and π-π Interactions in Luminescent Multinuclear Cyclometalated Platinum(II) Homologues Tethered by Oligophosphine Auxiliaries. *J. Am. Chem. Soc.* **2004**, *126*, 7639−7651. (j) Diez, A.; Fornies, J.; Fuertes, S.; Larraz, C.; Lalinde, E.; Lopez, J. A.; Martin, A.; Moreno, M. T.; Sicilia, V. Synthesis and Luminescence of Cyclometalated Compounds with Nitrile and Isocyanide Ligands. *Organometallics* **2009**, *28*, 1705−1718.

(3) (a) Rossi, E.; Murphy, L.; Brothwood, P. L.; Colombo, A.; Dragonetti, C.; Roberto, D.; Ugo, R.; Cocchid, M.; Williams, J. A. G. Cyclometallated Platinum(II) Complexes of 1,3-di(2-pyridyl)-Benzenes: Tuning Excimer Emission From Red to Near-Infrared for NIR-OLEDs. *J. Mater. Chem.* **2011**, *21*, 15501−15510. (b) Murphy, L.; Brulatti, P.; Fattori, V.; Cocchi, M.; Williams, J. A. G. Blue-Shifting the Monomer and Excimer Phosphorescence of Tridentate Cyclometallated Platinum(II) Complexes for Optimal White-Light OLEDs. *Chem. Commun.* **2012**, *48*, 5817−5819.

(4) (a) Chung, C. Y.-S.; Li, S. P.-Y.; Louie, M.-W.; Lo, K. K.-W.; Yam, V. W.-W. Induced Self-Assembly and Disassembly of Water-Soluble Alkynylplatinum(II) Terpyridyl Complexes with "Switchable" Near-Infrared (NIR) Emission Modulated by Metal−Metal Interactions Over Physiological pH: Demonstration of pH-Responsive NIR Luminescent Probes in Cell-Imaging Studies. *Chem. Sci.* **2013**, *4*, 2453−2462. (b) Chung, C. Y.-S.; Yam, V. W.-W. Selective Label-Free

Detection of G-Quadruplex Structure of Human Telomere by Emission Spectral Changes in Visible-and-NIR Region Under Physiological Condition Through the FRET of a Two-Component PPE-SO3⁻−Pt(II) Complex Ensemble with Pt/Pt, Electrostatic and π−π Interactions. *Chem. Sci.* **2013**, *4*, 377−387.

(5) Hill, M. G.; Bailey, J. A.; Miskowski, V. M.; Gray, H. B. Spectroelectrochemistry and Dimerization Equilibria of Chloro-(terpyridine)platinum(II). Nature of the Reduced Complexes. *Inorg. Chem.* **1996**, *35*, 4585−4590.

(6) (a) Chung, C. Y.-S.; Yam, V. W.-W. Induced Self-Assembly and Forster Resonance Energy Transfer studies of Alkynylplatinum(II) Terpyridine Complex Through Interaction With Water-Soluble Poly(phenylene ethynylene sulfonate) and the Proof-of-Principle Demonstration of this Two-Component Ensemble for Selective Label-Free Detection of Human Serum Albumin. *J. Am. Chem. Soc.* **2011**, *133*, 18775−18784. (b) Leung, S. Y.-L.; Tam, A. Y.-Y.; Tao, C.-H.; Chow, H. S.; Yam, V. W.-W. Single-Turn Helix-Coil Strands Stabilized by Metal···Metal and π-π Interactions of the Alkynylplatinum(II) Terpyridyl Moieties in meta-Phenylene Ethynylene Foldamers. *J. Am. Chem. Soc.* **2012**, *134*, 1047−1056. (c) Cong, Y.; Chan, K. H.-Y.; Keith, M.-C. W.; Yam, V. W.-W. Single-Stranded Nucleic Acid-Induced Helical Self- Assembly of Alkynylplatinum(II) Aerpyridyl Complexes. *Proc. Natl. Acad. Sci.* **2006**, *103*, 19652−19657. (d) Margaret, C.-L. Y.; Keith, M.-C. W.; Yuk, K. T. T.; Yam, V. W.-W. Aptamer-Induced Self-Assembly of a NIR-Emissive Platinum(II) Terpyridyl Complex for Label- and Immobilization-Free Detection of Lysozyme and Thrombin. *Chem. Commun.* **2010**, *46*, 7709−7711. (e) Margaret, C.-L. Y.; Yam, V. W.-W. NIR-Emissive Alkynylplatinum-(II) Terpyridyl Complex as a Turn-On Selective Probe for Heparin Quantification by Induced Helical Self-Assembly Behaviour. *Chem.—Eur. J.* **2011**, *17*, 11987−1990. (f) Cong, Y.; Chan, K. H.-Y.; Keith, M.-C. W.; Yam, V. W.-W. Polyelectrolyte-Induced Self-Assembly of Positively Charged Alkynylplatinum(II)−Terpyridyl Complexes in Aqueous Media. *Chem.—Eur. J.* **2008**, *14*, 4577−4584. (g) Chung, C. Y.-S.; Chan, K. H.-Y.; Yam, V. W.-W. Proof-of-Principle"Concept for Label-Free Detection of Glucose and a-Glucosidase activity Through the Electrostatic Assembly of Alkynylplatinum(II) Terpyridyl Complexes. *Chem. Commun.* **2011**, *47*, 2000−2002. (h) Wong, K. M.-C.; Yam, V. W.-W. Self-Assembly of Luminescent Alkynylplatinum(II) Terpyridyl Complexes: Modulation of Photophysical Properties Through Aggregation Behavior. *Acc. Chem. Res.* **2011**, *44*, 424−434. (i) Yam, V. W.-W.; Wong, K. M.-C.; Zhu, N. Solvent-Induced Aggregation Through Metal···Metal/π···π Interactions:Large Solvatochromism of Luminescent Organoplatinum(II) Terpyridyl Complexes. *J. Am. Chem. Soc.* **2002**, *124*, 6506−6507. (j) Po, C.; Tam, A. Y.-Y.; Wong, K. M.-C.; Yam, V. W.-W. Supramolecular Self-Assembly of Amphiphilic Anionic Platinum(II) Complexes: A Correlation between Spectroscopic and Morphological Properties. *J. Am. Chem. Soc.* **2011**, *133*, 12136−12143. (k) Yam, V. W.-W.; Chan, H.-Y.; Wong, K. M.-C.; Chu, B. W.-K. Luminescent Dinuclear Platinum(II) Terpyridine Complexes with a Flexible Bridge and "Sticky Ends. *Angew. Chem., Int. Ed.* **2006**, *45*, 6169−6173. (l) Chan, H.-Y.; Chow, H.-S.; Wong, K. M.-C.; Yeung, M. C.-L.; Yam, V. W.-W. Towards Thermochromic and Thermoresponsive Near-Infrared (NIR) Luminescent Molecular Materials Through the Modulation of Inter- and/or Intramolecular Pt/Pt and π−π Interactions. *Chem. Sci.* **2010**, *1*, 477−482. (m) Chung, C. Y.-S.; Yam, V. W.-W. Dual pH- and Temperature-Responsive Metallosupramolecular Block Copolymers with Tunable Critical Micelle Temperature by Modulation of the Self-Assembly of NIR-Emissive Alkynylplatinum(II) Complexes Induced by Changes in Hydrophilicity and Electrostatic Effects. *Chem.—Eur. J.* **2013**, *19*, 13182−13192. (n) Ni, J.; Zhang, X.; Wu, Y.-H.; Zhang, L.-Y.; Chen, Z.-N. Vapor- and Mechanical-Grinding-Triggered Color and Luminescence Switches for Bis(s-fluorophenylacetylide) Platinum(II) Complexes. *Chem.—Eur. J.* **2011**, *17*, 1171−1183.

(7) (a) Lai, S.-W.; Chan, M. C.-W.; Cheung, T.-C.; Peng, S.-M.; Che, C.-M. Probing d^8-d^8 Interactions in Luminescent Mono- and Binuclear Cyclometalated Platinum(II) Complexes of 6-Phenyl-2,2′-bipyridines. *Inorg. Chem.* **1999**, *38*, 4046−4055. (b) Ma, B.; Djurovich, P. I.; Thompson, M. E. Excimer and Electron Transfer Quenching Studies of a Cyclometalated Platinum Complex. *Coord. Chem. Rev.* **2005**, *249*, 1501−1510. (c) Gross, A.; Moriuchi, T.; Hirao, T. A Dinuclear Alkynylplatinum(II) Pyridinedicarboxamide: Conformational Change-Induced Switching of Emission Properties. *Chem. Commun.* **2013**, *49*, 1163−1165.

(8) (a) Kim, D.; Bredas, J.-L. Triplet Excimer Formation in Platinum-Based Phosphors: A Theoretical Study of the Roles of Pt-Pt Bimetallic Interactions and Interligand π-π Interactions. *Am. Chem. Soc.* **2009**, *131*, 11371−11380. (b) Stanislav, R.; Stoyanov, J. M.; Villegas, D.; Paul, R. Time-Dependent Density Functional Theory Study of the Spectroscopic Properties Related to Aggregation in the Platinum(II) Biphenyl Dicarbonyl Complex. *J. Inorg. Chem.* **2003**, *42*, 7852−7860.

(9) (a) Guerchais, V.; Fillaut, J.-L. Sensory Luminescent Iridium(III) and Platinum(II) Complexes for Cation Recognition. *Coord. Chem. Rev.* **2011**, *255*, 2448−2457. (b) Lanoe, P.-H.; Fillaut, J.-L.; Toupet, L.; Williams, J. A. G.; Le Bozec, H.; Guerchais, V. Cyclometallated Platinum(II) Complexes Incorporating Ethynyl−Favone Ligands: Switching Between Triplet and Singlet Emission Induced by Selective Binding of Pb^{2+} Ions. *Chem. Commun.* **2008**, 4333−4335. (c) Lanoe, P.-H.; Le Bozec, H.; Williams, J. A. G.; Fillaut, J.-L.; Guerchais, V. Cyclometallated Platinum(II) Complexes Containing Pyridyl-Acetylide Ligands: the Selective Influence of Lead Binding on Luminescence. *Dalton Trans.* **2010**, *39*, 707−710. (d) Latouche, C.; Lanoe, P.-H.; Williams, J. A. G.; Guerchais, V.; Boucekkine, A.; Fillaut, J.-L. Switching of Excited States in Cyclometalated Platinum Complexes Incorporating Pyridyl-Acetylide Ligands (Pt−CRC−py): a Combined Experimental and Theoretical Study. *New J. Chem.* **2011**, *35*, 2196−2202. (e) Fillaut, J.-L.; Akdas-Kilig, H.; Dean, E.; Latouche, C.; Boucekkine, A. Switching of Reverse Charge Transfers for a Rational Design of an OFF−ON Phosphorescent Chemodosimeter of Cyanide Anions. *Inorg. Chem.* **2013**, *52*, 4890−4897. (f) Savel, P.; Latouche, C.; Roisnel, T.; Akdas-Kilig, H.; Boucekkine, A.; Fillaut, J.-L. Cyclometalated Platinum(II) with Ethynyl-Linked Azobenzene Ligands: an Original Switching Mode. *Dalton Trans.* **2013**, *42*, 16773−16783.

(10) (a) Lo, H. S.; Yip, S. K.; Wong, K. M.-C.; Zhu, N.; Yam, V. W.-W. Selective Luminescence Chemosensing of Potassium Ions Based on a Novel Platinum(II) Alkynylcalix[4]crown-5 Complex. *Organometallics* **2006**, *25*, 3537−3540. (b) Tam, A. Y. Y.; Wong, K. M.-C.; Wang, G.; Yam, V. W.-W. Luminescent Metallogels of Platinum(II) Terpyridyl Complexes: Interplayof Metal···Metal, π−π and Hydrophobic−Hydrophobic Interactions on Gel Formation. *Chem. Commun.* **2007**, 2028−2030. (c) Po, C.; Ke, Z.; Tam, A. Y.-Y.; Chow, H.-F.; Yam, V. W.-W. A Platinum(II) Terpyridine Metallogel with an l-Valine-Modified Alkynyl Ligand: Interplay of Pt···Pt, p−p and Hydrogen-Bonding Interactions. *Chem.—Eur. J.* **2013**, *19*, 15735−15744.

(11) Lo, H.-S.; Yip, S.-K.; Zhu, N.; Yam, V. W.-W. The First Example of a Pt···Pt Interaction in Platinum(II) Complexes Bearing Bulky Tri-Tert-Butyl-2,2′:6′,2″-Terpyridine Pendants Via Conformational Control of the Calix[4]Arene Moiety. *Dalton Trans.* **2007**, *39*, 4386−4389.

(12) (a) Rice, S. F.; Gray, H. B. Electronic Absorption and Emission Spectra of Binuclear Platinum(I1) Complexes. Characterization of the Lowest Singlet and Triplet Excited States of $Pt_2(H_2P_20_5)_4^{-4}$. *J. Am. Chem. Soc.* **1983**, *105*, 4564−4571. (b) Kim, C. D.; Pillet, S.; Wu, G.; Fullagar, W. K.; Coppens, P. Excited-State Structure by Time-Resolved X-ray Diffraction. *Acta Crystallogr. A* **2002**, *58*, 133−137. (c) Novozhilova, I. V.; Volkov, A. V.; Coppens, P. Theoretical Analysis of the Triplet Excited State of the $[Pt_2(H_2P_2O_5)_4]^{4-}$ Ion and Comparison with Time-Resolved X-ray and Spectroscopic Results. *J. Am. Chem. Soc.* **2003**, *125*, 1079−1087. (d) Ozawa, Y.; Terashima, M.; Mitsumi, M.; Toriumi, K.; Yasuda, N.; Uekusa, H.; Ohashi, Y. Photoexcited Crystallography of Diplatinum Complex by Multiple-Exposure IP Method. *Chem. Lett.* **2003**, *32*, 62−63. (e) Stoyanov, S. R.; Villegas, J. M.; Rillema, D. P. Spectroscopic Properties of [Pt-2(mu-$P_2O_5H_2$)-(4)](4-): A Time-Dependent Density Functional Theory and Conductor-Like Polarizable Continuum Model Investigation. *J. Phys. Chem. B* **2004**, *108*, 12175−12180.

(13) ADF2013. *SCM Theoretical Chemistry*; Vrije Universiteit: Amsterdam, The Netherlands, http://www.scm.com.

(14) (a) Lee, C.; Yang, W.; Parr, R. G. Development of the Colle-Salvetti Correlation-Energy Formula Into a Functional of the Electron Density. *Phys. Rev. B* **1988**, *37*, 785−789. (b) Becke, A. D. Density-Functional Exchange-Energy Approximation with Correct Asymptotic Behavior. *Phys. Rev. A* **1988**, *38*, 3098−3100.

(15) (a) Grimme, S.; Antony, J.; Ehrlich, S.; Krieg, H. A Consistent and Accurate ab Initio Parametrization of Density Functional Dispersion Correction (DFT-D) for the 94 Elements H-Pu. *J. Chem. Phys.* **2010**, *132*, 154104−154123. (b) Grimme, S.; Ehrlich, S.; Goerigk, L. Effect of the Damping Function in Dispersion Corrected Density Functional Theory. *J. Comput. Chem.* **2011**, *32*, 1456−1465.

(16) (a) Van Lenthe, E.; Baerends, E. J.; Snijders, J. G. Relativistic Regular Two-Component Hamiltonians. *J. Chem. Phys.* **1993**, *99*, 4597−4610. (b) Van Lenthe, E.; Baerends, E. J.; Snijders, J. G. Relativistic Total Energy Using Regular Approximations. *J. Chem. Phys.* **1994**, *101*, 9783−9792. (c) Van Lenthe, E.; Ehlers, A.; Baerends, E. J. Geometry Optimization in the Zero Order Regular Approximation for Relativistic Effects. *J. Chem. Phys.* **1999**, *110*, 8943−8953.

(17) (a) Klamt, A.; Schürmann, G. COSMO: A New Approach to Dielectric Screening in Solvents with Explicit Expressions for the Screening Energy and its Gradient. *J. Chem. Soc.* **1993**, *2*, 799−805. (b) Klamt, A. Conductor-Like Screening Model for Real solvents: A New Approach to the Quantitative Calculation of Solvation Phenomena. *J. Phys. Chem.* **1995**, *99*, 2224−2235. (c) Klamt, A.; Jones, V. Treatment of the Outlying Charge in Continuum Solvation Models. *J. Chem. Phys.* **1996**, *105*, 9972−9981. (d) Klamt, A.; Jones, V.; Bürger, T.; Lohrenz, J. C. Refinement and Parametrization of COSMO-RS. *J. Phys. Chem. A* **1998**, *102*, 5074−5085.

(18) (a) Perdew, J. P.; Burke, K.; Ernzerhof, M. Generalized Gradient Approximation Made Simple. *Phys. Rev. Lett.* **1996**, *77*, 3865−3868. (b) Adamo, C.; Barone, V. Toward Reliable Density Functional Methods Without Adjustable Parameters: The PBE0 model. *J. Chem. Phys.* **1999**, *110*, 6158−6170.

(19) Hay, P. J.; Wadt, W. R. Ab Initio Effective Core Potentials for Molecular Calculations - Potentials for the Transition-Metal Atoms Sc to Hg. *J. Chem. Phys.* **1985**, *82*, 270−283.

(20) Frisch, M. J.; Trucks, G. W.; Schlegel, H. B.; Scuseria, G. E.; Robb, M. A.; Cheeseman, J. R.; Scalmani, G.; Barone, V.; Mennucci, B.; Petersson, G. A.; et al. *Gaussian09*, Revision D. 01; Gaussian Inc.: Pittsburgh, PA, 2009.

(21) Tomasi, J.; Mennucci, B.; Cammi, R. Quantum Mechanical Continuum Solvation Models. *Chem. Rev.* **2005**, *105*, 2999−3093.

(22) Macrae, C. F.; Bruno, I. J.; Chisholm, J. A.; Edgington, P. R.; McCabe, P.; Pidcock, E.; Rodriguez-Monge, L.; Taylor, R.; van de Streek, J.; Wood, P. A. Mercury CSD 2.0. *J. Appl. Crystallogr.* **2008**, *41*, 466−470.

(23) Dennington, R.; Keith, T.; Millam, J. *GaussView*, Version5; Semichem Inc.: Shawnee Mission, KS, 2009.

(24) Gorelsky, S. I., *Swizard* program, revision 4.5, http://www-sg-chem.net/swizard.

(25) Gorelsky, S. I. *AOMix* program, http://www.sg-chem.net/AOMix.

(26) Chai, J.-D.; Head-Gordon, M. Long-Range Corrected Hybrid Density Functionals with Damped Atom−Atom Dispersion Corrections. *Phys. Chem. Chem. Phys.* **2008**, *10*, 6615−6620.